ACS Catalysis

Research Article

pubs.acs.org/acscatalysis

Magnetically Separable Microporous Fe−Porphyrin Networks for Catalytic Carbene Insertion into N−H Bonds

Jin Yoo,[†,∥] Nojin Park,[†,∥] Joon Hyun Park,[†] Ji Hoon Park,[†] Sungah Kang,[†] Sang Moon Lee,[†] Hae Jin Kim,[‡] Hyein Jo,[§] Je-Geun Park,[§] and Seung Uk Son*[,†]

[†]Department of Chemistry and Department of Energy Science, Sungkyunkwan University, Suwon 440-746, Korea

[‡]Korea Basic Science Institute, Daejeon 350-333, Korea

[§]Department of Physics & Astronomy, Seoul National University, Seoul 151-747, Korea

Supporting Information

ABSTRACT: Microporous organic networks (MONs) are a new class of porous materials. This work shows the application of MON chemistry for the preparation of magnetically separable catalytic systems. By the Sonogashira coupling of Fe^{III}−tetrakis(4-ethynylphenyl)porphyrin and 1,4-diiodobenzene, Fe_3O_4 nanoparticles were coated successfully with Fe−porphyrin networks. The average thickness of the homogeneous coating was ∼17 nm. According to the powder X-ray diffraction and N_2 isotherm analyses, the Fe−porphyrin network coating exhibited amorphous and microporous characteristics. The microporous Fe−porphyrin networks on the Fe_3O_4 nanoparticles showed good catalytic performance for carbene insertion into the N−H bond of amines. The catalytic systems were easily recycled from the reaction mixture by magnetic separation. We believe that the synthetic strategy in this work can be extended to the various catalytic systems.

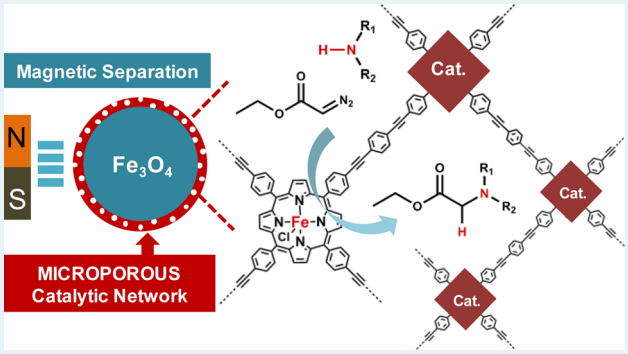

KEYWORDS: *microporous organic polymer, magnetic nanocatalyst, porphyrin, iron, carbene insertion*

INTRODUCTION

During the past decade, catalytic systems based on magnetic nanosupports have constituted a fast-growing research field.[1] In the catalytic chemical transformations, the magnetic separation of catalysts is a very attractive workup method, because of its ease and rapidity. To graft the catalytic components on the magnetic supports, various strategies have been applied. First, single-molecule catalytic moieties having polar[2] or polyaromatic[3] anchoring groups were prepared and loaded on the surface of magnetic nanoparticles. Second, the catalysts were fixed tightly on the graphitic carbon layer of magnetic nanoparticles through carbon−carbon bond formation based on diazonium chemistry.[4] Third, nanocatalysts were deposited on the magnetic supports.[5] Fourth, polymer layers such as polystyrene shells were formed on the magnetic nanoparticles and then the catalytic species were further introduced by a postsynthetic approach.[6] In this case, chemical modification is difficult and the catalytic performance of the inner building blocks is poor because of nonporosity. Recently, polymer- and dendrimer-coated magnetic nanoparticles and their catalytic applications were reviewed by Reiser et al.[7] However, *porous* polymeric networks on the surface of magnetic particles have been relatively less explored.[8]

Recently, microporous organic networks (MONs) have become an important class of porous materials.[9] The networking of the rigid building blocks through robust covalent bonds induced the microporosity of materials. By designing the functional building blocks including porphyrins, tailored catalytic functionalities can be achieved in MONs.[10,11] The porphyrins are very versatile chemical species for diverse applications.[12] Especially, various metalloporphyrins have shown interesting catalytic performance via the interaction of substrates with central metal ions.[13] Among the metalloporphyrins, iron porphyrins are expanding the range of catalytic applications.[14] It is noteworthy that the nontoxic property of iron and its abundance in the earth's crust have triggered research on the new catalytic performance of various iron complexes.[15] Although microporous or macroporous organic materials bearing porphyrin moieties have been reported,[11] as far as we are aware, porphyrin networks on the magnetic supports have not been reported.

The Cooper group and others have reported the synthesis of microporous organic polymers by the Sonogashira coupling of multialkynes and multihalides.[16] Our research group has studied the synthesis of new functional MONs based on Sonogashira coupling.[17] Recently, we verified the successful

Received: September 12, 2014
Revised: November 1, 2014
Published: December 2, 2014

   dx.doi.org/10.1021/cs501378j | ACS Catal. 2015, 5, 350−355

coating of MONs on various solid supports.[18] In this work, we report the synthesis of Fe−porphyrin microporous networks on iron oxide nanoparticles (Fe_3O_4@**FePMN**) and their catalytic performance for carbene insertion reaction into N−H bonds.

EXPERIMENTAL SECTION

Scanning and transmission electron microscopy were conducted using JSM6700F and a JEOL 2100F units, respectively. N_2 isotherms were recorded at 77 K using a BELSORP II-mini adsorption equipment. Powder X-ray diffraction patterns were obtained using a Rigaku MAX-2200 instrument. Elemental analysis was performed using a CE EA1110 elemental analyzer. Infrared absorption spectra were recorded using a Bruker VERTEX 70 FT-IR spectrometer. The magnetic properties were measured using a Quantum Design MPMS XL SQUID magnetometer. X-ray photoelectron spectroscopy was conducted using a Thermo VG spectrometer. ^{1}H and ^{13}C NMR spectra were recorded using a 500 MHz Varian spectrometer. Inductively coupled plasma-atomic emission spectroscopy was performed using a Shimadzu ICPS-1000IV instrument. The mass spectrum was obtained using a JEOL JMS 700 spectrometer.

Preparation of $Fe^{III}Cl$−Porphyrin Building Block.[19] 5,10,15,20-Tetrakis(4-ethynylphenyl)porphyrin was prepared following the literature method.[19a] For the preparation of $Fe^{III}Cl$−5,10,15,20-tetrakis(4-ethynylphenyl)porphyrin,[19c] $FeCl_3$ (0.52 g, 0.32 mmol) and 5,10,15,20-tetrakis(4-ethynylphenyl)porphyrin (0.23 g, 0.32 mmol) were dissolved in DMF (35 mL) in a 50 mL Schlenk flask under argon. The reaction mixture was refluxed for 12 h. After it was cooled to room temperature, the reaction mixture was poured into 6 N HCl solution (100 mL). After the mixture was shaken for 3 min, the solid was isolated by centrifugation. The product was extracted using methylene chloride and 3 N HCl solution. After the methylene chloride extract was dried with anhydrous $MgSO_4$, the solvent was evaporated. After the solid was dissolved in DMF (1 mL), the solution was poured into hexane (15 mL) in a 20 mL vial. The solid was separated by centrifugation, washed with hexane, and dried under vacuum. Crystals were obtained by diffusing pentane into an ether solution of product (yield: 59%). The coordination of $Fe^{III}Cl$ was confirmed by shfiting of the Q bands[19b,20] from 516, 551, 590, and 660 nm to 512, 579, and 690 nm and high-resolution mass spectroscopy (HRMS for $[M - Cl]^+$, $[C_{52}H_{28}N_4Fe]^+$, calcd 764.1663, obsd 764.1666).

Preparation of Fe_3O_4@FePMN. The Fe_3O_4 nanoparticles were prepared following the literature method.[21] In a flame-dried 50 mL Schlenk flask equipped with a condenser, Fe_3O_4 nanospheres (0.30 g) were dispersed in diisopropylamine (45 mL) under argon with sonication for 30 min. $Pd(PPh_3)_2Cl_2$ (4.2 mg, 6.3 μmol) and CuI (1.2 mg, 6.3 μmol) were added to the reaction mixture. Then, the reaction mixture was sonicated for 1 h and stirred for a further 1 h without sonication. $Fe^{III}Cl$−5,10,15,20-tetrakis(4-ethynylphenyl)porphyrin (48 mg, 0.060 mmol) and 1,4-diiodobenzene (40 mg, 0.12 mmol) in DMF (3 mL) were added to the solution. The reaction mixture was heated to 90 °C for 24 h. After the mixture was cooled to room temperature, the solid was isolated by centrifugation, washed with acetone, CH_2Cl_2, and diethyl ether, and dried under vacuum. The amount of product obtained was 0.33 g (~92%).

Fe_3O_4 Etching from Fe_3O_4@FePMN. In a 30 mL vial, Fe_3O_4@**FePMN** (0.30 g) was added to a 6 N HCl solution (15 mL) at room temperature. The reaction mixture was stirred for 20 min. The solid was isolated by centrifugation, washed with water and methanol, and dried under vacuum.

Catalytic Tests. In a flame-dried 20 mL Schlenk tube, Fe_3O_4@**FePMN** (13.5 mg, 2.4 μmol of Fe−porphyrins based on elemental analysis) was added to amine (0.24 mmol) in acetone (3 mL) under argon. Ethyl diazoacetate (0.24 mmol, 0.20 mL of a 15% solution in toluene) was added to the reaction mixture. After it was stirred for 20 min at room temperature, the solution was decanted into a vial and the catalysts were separated using a magnet. Using 1,4-dimethoxybenzene as an internal standard, the solution was analyzed by 500 MHz ^{1}H NMR spectroscopy. To obtain the isolated yields, the solvent was evaporated and the products were purified by flash column chromatography. All of the products in Table 1 are known compounds,[22] and their structures were confirmed by ^{1}H and ^{13}C NMR spectroscopy (Figure S1 in the Supporting Information).

RESULTS AND DISCUSSION

Scheme 1 shows the synthetic route for magnetically separable microporous Fe−porphyrin networks.

Scheme 1. Synthesis of Fe−Porphyrin Microporous Networks on the Fe_3O_4 Nanoparticles (Fe_3O_4@FePMN)

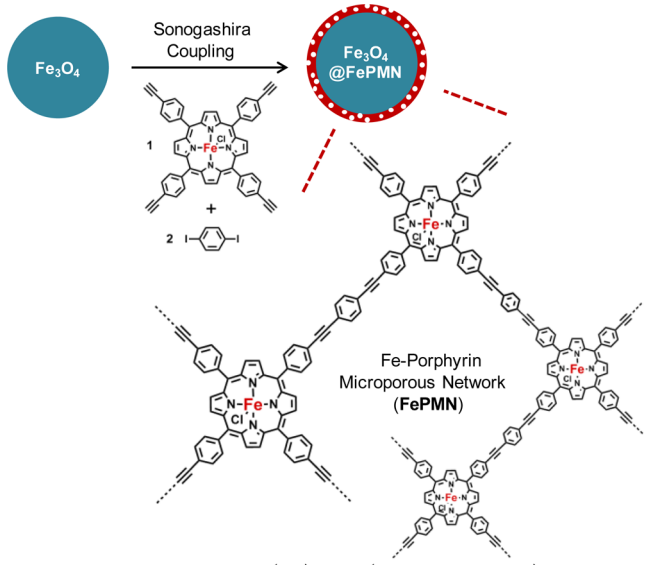

As a building block, Fe^{III}−tetrakis(4-ethynylphenyl)-porphyrin was prepared following the literature method.[19] Iron oxide (Fe_3O_4) nanospheres with an average diameter of 190 nm (aggregates of 30−50 nm nanoparticles) were prepared by the solvothermal method.[21] Using 1,4-diiodobenzene as a coupling partner, the Fe_3O_4 nanoparticles were coated with Fe−porphyrin networks by Sonogashira coupling (see the Experimental Section for the optimized experimental conditions). The resultant Fe_3O_4@**FePMN** materials were investigated by scanning electron microscopy (SEM) and transmission electron microscopy (TEM). (Figure 1)

In the SEM and TEM analysis, the homogeneous coating of Fe−porphyrin networks on the Fe_3O_4 nanoparticles was clearly observed (Figure 1b,c,e,f). The average coating thickness was ~17 nm. When 0.30 g of Fe_3O_4 and 48 mg of Fe^{III}−tetrakis(4-ethynylphenyl)porphyrin building blocks were used for the Sonogashira coupling, a homogeneous coating was observed.

dx.doi.org/10.1021/cs501378j | ACS Catal. 2015, 5, 350−355

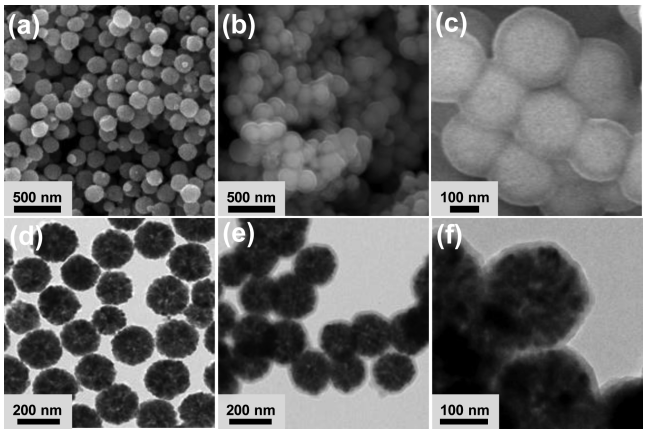

Figure 1. SEM and TEM images of the bare Fe_3O_4 (a, d) and Fe_3O_4@**FePMN** (b, c, e, f).

When the amount of Fe_3O_4 decreased from that in the optimized experimental conditions or the amount of Fe–porphyrin building block increased, polymeric materials that formed separately were observed as impurities. The Fe_3O_4@**FePMN** materials were investigated by N_2 sorption isotherm analysis on the basis of the Brunauer–Emmett–Teller (BET) theory and powder X-ray diffraction studies (PXRD) (Figure 2).

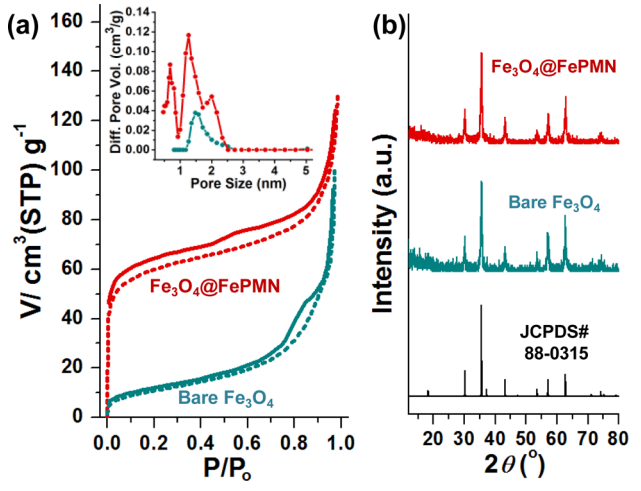

Figure 2. (a) N_2 adsorption (dotted line)–desorption (solid line) isotherms at 77 K and pore size distribution diagrams based on the DFT method for adsorption isotherms (inset: bare Fe_3O_4, green; Fe_3O_4@**FePMN**, red). (b) PXRD patterns of the bare Fe_3O_4 (green) and Fe_3O_4@**FePMN** (red).

As shown in Figure 2a, the bare Fe_3O_4 showed poor porosity with a surface area of 40 m^2/g. In comparison, Fe_3O_4@**FePMN** showed a typical microporosity with an increased surface area of 173 m^2/g, which is attributed to the formation of microporous organic networks on the surface of Fe_3O_4. According to the PXRD studies, the crystalline nature of the Fe_3O_4 was retained after coating with Fe–porphyrin networks (Figure 2b). The PXRD pattern matched well with that of cubic Fe_3O_4 (JCPDS# 88–0315). According to the elemental analysis via combustion, the N, C, and H contents in the Fe_3O_4@**FePMN** were 1.00, 13.81, and 0.90 wt %, respectively, which matched well with the expected chemical compositions (building block ratio Fe–porphyrin:phenyl = 1:2; theoretical chemical component of $Fe^{III}Cl$–porphyrin network $C_{52}N_4H_{24}FeCl + 2C_6H_4$; calculated composition of N, C, and H in networks N 1.01, C 13.81, H 0.58 wt %, respectively). On the basis of the N wt %, the content of Fe–porphyrins in the materials was calculated as 0.18 mmol/g. Considering the N, C, and H composition (total 15.7 wt %) from elemental analysis and theoretical chemical component (additional 1.6 wt % of Fe and Cl), the content of Fe–porphyrin networks in Fe_3O_4@**FePMN** was calculated as ~17 wt %.

For further analysis of the Fe–porphyrin networks on the surface of Fe_3O_4 nanospheres, the inner Fe_3O_4 was completely etched by treatment with 6 N HCl solution (Figure 3a). The obtained hollow porphyrin networks (**H-FePN**)[23] were investigated by SEM and TEM analysis.

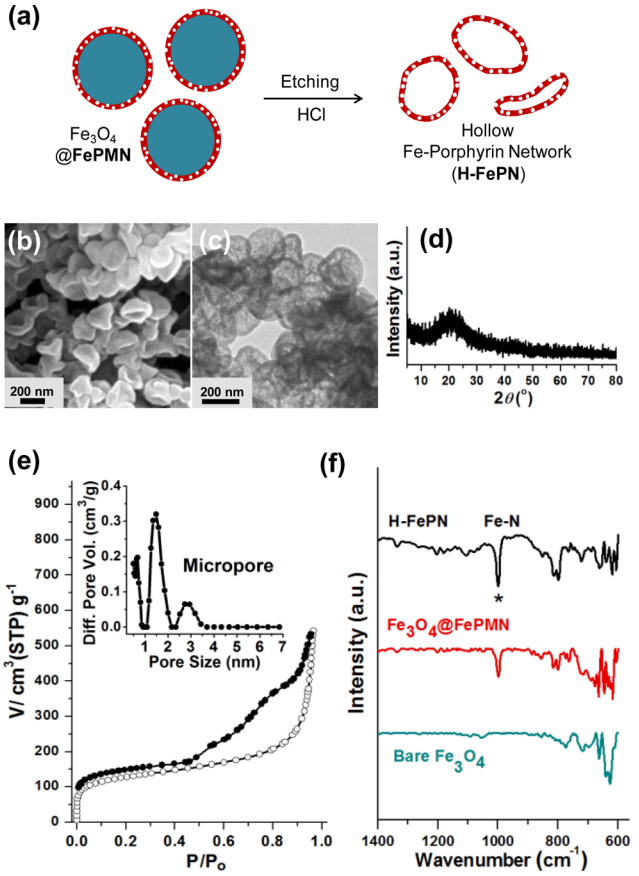

Figure 3. (a) Hollow porphyrin networks (**H-FePN**) formed via the Fe_3O_4 etching with HCl solution. (b) SEM, (c) TEM, and (d) PXRD patterns. (e) N_2 sorption isotherm of **H-FePN** at 77 K and pore size distribution diagrams (inset) by the DFT method. (f) IR absorption spectra of **H-FePN**, Fe_3O_4@**FePMN**, and bare Fe_3O_4. The sharp peak at 999 cm^{-1} indicated by an asterisk corresponds to the Fe–N vibration.[19b]

As shown in Figure 3b,c, the **H-FePN** materials showed a hollow nature. SEM analysis showed that the hollow materials were distorted from a spherical shape due to the empty inner space of the materials. In the TEM analysis, the empty inner space was clearly observed (Figure 3c). The thicknesses of the hollow materials were found to be in a range of 15–20 nm, which matched well with the thickness of the Fe–porphyrin network in Fe_3O_4@**FePMN**. The PXRD pattern of **H-FePN** showed an amorphous characteristic, which has been commonly observed in microporous organic materials prepared

dx.doi.org/10.1021/cs501378j | ACS Catal. 2015, 5, 350–355

by Sonogashira coupling[14] (Figure 3d). The analysis of the N_2 sorption isotherm of **H-FePN** showed microporous and mesoporous characteristics with a surface area of 452 m^2/g (Figure 3e and Figure S2 in the Supporting Information and inset) The mesopores of **H-FePN** resulted from the inner Fe_3O_4 nanospheres (aggregates of 30−50 nm Fe_3O_4 nanoparticles) of Fe_3O_4**@FePMN**. Unfortunately, solid-phase nuclear magnetic resonance (NMR) spectroscopy could not be applied to **H-FePN** due to the paramagnetic nature of Fe^{III}−porphyrin moieties. The infrared (IR) absorption spectra of **H-FePN** and Fe_3O_4**@FePMN** showed a characteristic peak at 999 cm^{-1} which corresponds to the vibration frequency of Fe−N bonds of Fe^{III}Cl−porphyrins[17b] (Figure 3f). As expected, the IR spectrum of Fe_3O_4**@FePMN** contained vibrations from both **H-FePN** and bare Fe_3O_4 (Figure 3f). On consideration of these findings, the analysis of **H-FePN** materials confirmed that the coating on the Fe_3O_4 resulted from the microporous networking of porphyrin building blocks.

Next, the magnetic nature of Fe_3O_4**@FePMN** materials was investigated using a superconducting quantum interference device (SQUID). The magnetic hysteresis loop of Fe_3O_4**@FePMN** measured at 300 K showed typical superparamagnetic characteristics and 81 emu/g of the saturation magnetization (M_s) (Figure 4a). In view of the M_s values (4−60 emu/g) of

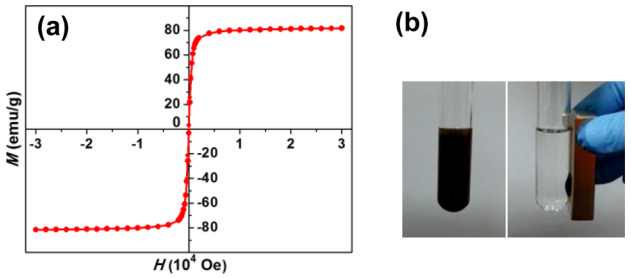

Figure 4. (a) Magnetic hysteresis loop of Fe_3O_4**@FePMN** measured at 300 K. (b) Photographs of magnetic separation of Fe_3O_4**@FePMN** from acetone solution using a magnet.

the magnetic catalytic systems in the literature,[1−8] the magnetic properties of Fe_3O_4**@FePMN** materials are quite promising for magnetic separation. As shown in Figure 4b, the Fe_3O_4**@FePMN** materials were retrieved easily from the reaction mixture using a magnet. Thus, we applied the materials as magnetically separable catalysts in organic transformations.

Recently, transition-metal catalysts for carbene insertion into N−H bonds have attracted significant attention.[24] In these studies, diazo compounds such as ethyl diazoacetate (EDA) have been used as a carbene precursor.[24] Most studies were conducted in homogeneous systems, including asymmetric versions.[24] Fe^{III}Cl−porphyrin complexes are known to catalyze carbene insertion into N−H bonds.[22] However, as far as we are aware, efficient heterogeneous systems for this chemical conversion have not been reported.

Table 1 summarizes the results of the catalytic performance of Fe_3O_4**@FePMN** materials for carbene insertion into N−H bonds. On the basis of elemental analysis, 1 mol % of Fe−porphyrin moieties in Fe_3O_4**@FePMN** was used for the reaction (see the Experimental Section for a detailed procedure). In our tests, when no catalysts or the bare Fe_3O_4 nanoparticles were used instead of Fe_3O_4**@FePMN**, no conversions of the EDA were observed (entries 1 and 2 in Table 1). According to the reaction time screening, the

Table 1. Catalytic Carbene Insertion into N−H Bonds by Fe_3O_4@FePMN[a]

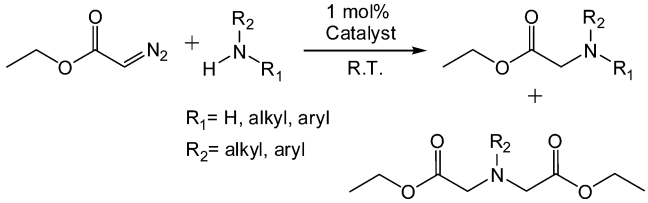

entry	amine	time (min)	yield[b] (%)	S[c] (%)
1[d]	piperidine	20	0	
2[e]	piperidine	20	0	
3	piperidine	5	42	100/−/0
4	piperidine	10	76	100/−/0
5	piperidine	15	96	100/−/0
6	piperidine	20	100 (98)	100/−/0
7[f]	piperidine	20	0	
8[g]	piperidine	20	100	100/−/0
9[h]	piperidine	20	100	100/−/0
10[i]	piperidine	20	100	100/−/0
11	*N,N*-diethylamine	20	91 (74)[j]	100/−/0
12	*tert*-butylamine	20	42	67/32/1
13	4-methoxyaniline	20	100[k]	83/16/1
14	aniline	20	100 (94)	97/2/1
15	4-bromoaniline	20	100 (96)	98/1/1
16	4-nitroaniline	20	81 (48)[l]	76/2/22

[a]Reaction conditions: Fe_3O_4**@FePMN** catalyst (1 mol % of Fe−porphyrins of substrates, 13.5 mg, 2.4 μmol of Fe−porphyrins based on the elemental analysis for N content), EDA (0.24 mmol, 0.20 mL of 15% solution in toluene), amine (0.24 mmol), acetone (3 mL), argon, room temperature. [b]Conversion yields of EDA using ^{1}H NMR spectroscopy. 1,4-Dimethoxybenzene was used as an internal standard. The isolated yields of the major products after column chromatography are indicated in parentheses. [c]Selectivity: molar ratios of single N−H insertion product, double N−H insertion product, and the dimerization product of EDA. [d]No catalyst was used. [e]Fe_3O_4 nanoparticles (13.5 mg) were used as catalysts. [f]After reaction with the same setup as in entry 9, the catalyst was completely removed. After addition of EDA (0.24 mmol) and piperidine (0.24 mmol) to the solution, the reaction was conducted for an additional 20 min, and further conversion was measured. [g]The catalysts recovered from entry 6 were used. [h]The catalysts recovered from entry 8 were used. [i]The catalysts recovered from entry 9 were used. [j]The product was volatile under vacuum-drying, resulting in the loss of the isolated products. [k]Unfortunately, the product was unstable and decomposed during column chromatography. [l]Because of the significant formation of EDA dimer, the maximum isolated yield of the major product was calculated as 50%.

conversion of EDA into the N−H insertion product of piperidine was completed within 20 min in acetone (entries 3−6 in Table 1).[25] Other byproducts such as an EDA dimer were not detected in the conversion. After column chromatography, 98% of the N−H insertion product of piperidine was isolated, indicating the high selectivity of the reaction.[26]

When the catalysts recovered from the first run were used in the second run, 100% conversion of EDA to the N−H inserted product was observed. The recovery tests showed further complete conversion in the successive third and fourth runs (entries 8−10 in Table 1). The catalysts recovered from the fourth run were investigated by TEM, PXRD, and X-ray photoelectron (XPS) spectroscopy. As shown in Figure 5a,b, the Fe−porphyrin coating was completely retained. The PXRD pattern (Figure 5c) and XPS spectra (Figure 5d) supported the

dx.doi.org/10.1021/cs501378j | ACS Catal. 2015, 5, 350−355

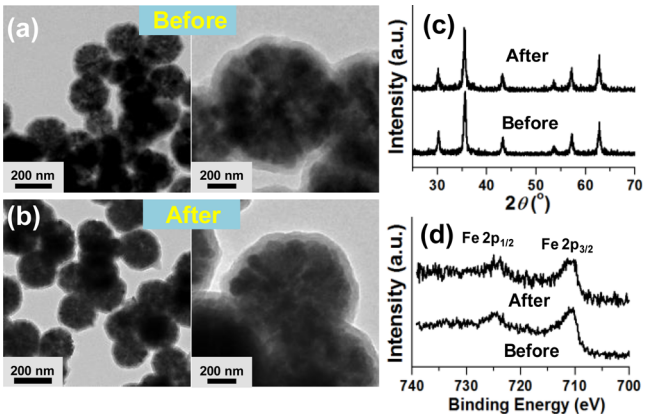

Figure 5. (a, b) TEM images, (c) PXRD patterns, and (d) XPS spectra of Fe_3O_4@**FePMN** catalysts before reaction and after four runs. The difference in signal/noise degrees in the PXRD patterns and XPS spectra resulted from the different amounts of samples.

retention of the physicochemical properties of the catalysts. In the XPS spectra, two major Fe $2p_{3/2}$ orbital peaks appeared at 711.2 and 710.3 eV, which were assigned to Fe ions in $Fe^{III}Cl$–porphyrin and Fe_3O_4, respectively. The Fe $2p_{3/2}$ orbital peaks of Fe ions in $Fe^{III}Cl$–5,10,15,20-tetraphenylporphyrin and Fe_3O_4 are known to appear at 711.2 and 710.2 eV, respectively.[27]

To investigate the heterogeneous nature of catalytic action of Fe_3O_4@**FePMN**, we conducted control experiments as follows. First, after the first run, the catalysts were removed, and the reaction mixture was obtained. The possible Fe leaching into the reaction mixture was investigated by inductively coupled plasma-atomic emission spectroscopy (ICP-AES). Fe was not detected in a range of a reliable detection limit (>0.2 ppm for Fe ions).[28] Second, after the first run in another setup, the catalysts were completely removed, and then EDA and amine were added to the reaction mixture. According to ^{1}H NMR studies on the reaction mixture obtained after an additional 20 min, the conversion of EDA stopped completely with the removal of catalysts, implying that the catalytic reaction by Fe_3O_4@**FePMN** proceeded in a heterogeneous fashion (entry 7 in Table 1).

The catalytic activities of the Fe_3O_4@**FePMN** systems were further investigated toward diverse substrates. Another secondary amine, *N*,*N*-diethylamine, showed a good conversion with a perfect selectivity (entry 11 in Table 1). When primary amines were used, a selectivity problem was encountered. In particular, electron-rich primary amines such as *tert*-butylamine and 4-methyoxyaniline resulted in a mixture of single and double N–H insertion products (16–32%) (entries 12 and 13 in Table 1). Interestingly, the single N–H insertion product of 4-methoxyaniline was relatively unstable and decomposed during column chromatography. When aniline and 4-bromoaniline were used, the single N–H insertion products were formed dominantly and were isolated in excellent yields by column chromatography (entries 14 and 15 in Table 1). In the case of 4-nitroaniline substrate, although the single N–H insertion product was quite stable, only a 48% isolated yield was obtained (entry 16 in Table 1). A longer reaction time did not significantly increase the isolated yield, which was attributed to the formation of EDA dimer. Fe–porphyrins are known to catalyze the dimerization of EDA in the absence of carbene acceptors.[22] Moreover, the relatively slow reaction kinetics for carbene insertion into the N–H bond of 4-nitroaniline has been reported in the literature.[22]

CONCLUSION

Magnetically separable catalytic systems were developed by the coating of microporous Fe–porphyrin networks on Fe_3O_4 nanoparticles. After the inner Fe_3O_4 materials were etched, the PXRD and N_2 isotherm analyses of the Fe–porphyrin networks showed amorphous and microporous character of the Fe–porphyrin coating. The resultant catalytic system showed good catalytic performance for carbene insertion into the N–H bond of amines. This work shows that MON chemistry can be applied as a new loading method of catalytic moieties on the magnetic supports. We believe that more diverse magnetically separable catalytic systems can be developed on the basis of the synthetic strategy in this work.

ASSOCIATED CONTENT

Supporting Information

The following file is available free of charge on the ACS Publications website at DOI: 10.1021/cs501378j.

^{1}H and ^{13}C NMR spectra of products and pore size distribution diagram of **H-FePN** (PDF)

AUTHOR INFORMATION

Corresponding Author

*E-mail for S.U.S.: sson@skku.edu.

Author Contributions

‖These authors (J.Y. and N.P.) contributed equally.

Notes

The authors declare no competing financial interest.

ACKNOWLEDGMENTS

This work was supported by Grant No. NRF-2012-R1A2A2A01045064 (Midcareer Researcher Program) through the National Research Foundation of Korea and by Grant No. 10047756 (Technology Innovation Program) funded by the Ministry of Trade, Industry & Energy of Korea. Magnetization measurements were carried out at the Center for Correlated Electron Systems, Institute for Basic Science (IBS).

ABBREVIATIONS

TEM, transmission electron microscopy; SEM, scanning electron microscopy; NMR, nuclear magnetic resonance; PXRD, powder X-ray diffraction; XPS, X-ray photoelectron spectroscopy; EDS, energy dispersive X-ray absorption spectroscopy; ICP-AES, inductively coupled plasma atomic emission spectroscopy; BET, Brunauer–Emmett–Teller; DFT, density functional theory; SQUID, superconducting quantum interference device; MON, microporous organic network; FePMN, Fe–porphyrin microporous network; EDA, ethyl diazoacetate

REFERENCES

(1) Reviews on the magnetically separable catalysts: (a) Wang, D.; Astruc, D. *Chem. Rev.* **2014**, *114*, 6949–6985. (b) Polshettiwar, V.; Luque, R.; Fihri, A.; Zhu, H.; Bouhrara, M.; Basset, J.-M. *Chem. Rev.* **2011**, *111*, 3036–3075. (c) Shylesh, S.; Schünemann, V.; Thiel, W. R. *Angew. Chem., Int. Ed.* **2010**, *49*, 3428–3459.

(2) Selected examples: (a) Hu, A.; Yee, G. T.; Lin, W. *J. Am. Chem. Soc.* **2005**, *127*, 12486–12487. (b) Ding, S.; Xing, Y.; Radosz, M.;

Shen, Y. *Macromolecules* **2006**, *39*, 6399−6405. (c) Li, P.; Wang, L.; Zhang, L.; Wang, G.-W. *Adv. Synth. Catal.* **2012**, *354*, 1307−1318.
(3) (a) Wittmann, S.; Schätz, A.; Grass, R. N.; Stark, W. J.; Reiser, O. *Angew. Chem., Int. Ed.* **2010**, *49*, 1867−1870. (b) Keller, M.; Collière, V.; Reiser, O.; Caminade, A.-M.; Majoral, J.-P.; Quali, A. *Angew. Chem., Int. Ed.* **2013**, *52*, 3626−3629.
(4) (a) Grass, R. N.; Athanassiou, E. K.; Stark, W. J. *Angew. Chem., Int. Ed.* **2007**, *46*, 4909−4912. (b) Schätz, A.; Grass, R. N.; Stark, W. J.; Reiser, O. *Chem. Eur. J.* **2008**, *14*, 8262−8266. (c) Schätz, A.; Grass, R. N.; Kainz, Q.; Stark, W. J.; Reiser, O. *Chem. Mater.* **2010**, *22*, 305−310. (d) Kainz, Q. M.; Linhardt, R.; Maity, P. K.; Hanson, P. R.; Reiser, O. *ChemSusChem* **2013**, *6*, 721−729. (e) Schätz, A.; Long, T. R.; Grass, R. N.; Stark, W. J.; Hanson, P. R.; Reiser, O. *Adv. Funct. Mater.* **2010**, *20*, 4323−4328.
(5) Selected examples: (a) Zhu, M.; Diao, G. *J. Phys. Chem. C* **2011**, *115*, 24743−24749. (b) Linhardt, R.; Kainz, Q. M.; Grass, R. N.; Stark, W. J.; Reiser, O. *RSC Adv.* **2014**, *4*, 8541−8549. (e) Kainz, Q. M.; Linhardt, R.; Grass, R. N.; Vilé, G.; Pérez-Ramírez, J.; Stark, W. J.; Reiser, O. *Adv. Funct. Mater.* **2014**, *24*, 2020−2027. (c) Laska, U.; Frost, C. G.; Price, G. J.; Plucinski, P. K. *J. Catal.* **2009**, *268*, 318−328. (d) Kim, Y.; Kim, M.-J. *Bull. Korean Chem. Soc.* **2010**, *31*, 1368−1370.
(6) Stevens, P. D.; Fan, J.; Gardimalla, H. M. R.; Yen, M.; Gao, Y. *Org. Lett.* **2005**, *7*, 2085−2088.
(7) Kainz, Q. M.; Reiser, O. *Acc. Chem. Res.* **2014**, *47*, 667−677.
(8) Yang, X.; Li, B.; Majeed, I.; Liang, L.; Long, X.; Tan, B. *Polym. Chem.* **2013**, *4*, 1425−1429.
(9) (a) Dawson, R.; Cooper, A. I.; Adams, D. J. *Prog. Polym. Sci.* **2012**, *37*, 530−563. (b) Vilela, F.; Zhang, K.; Antonietti, M. *Energy Environ. Sci.* **2012**, *5*, 7819−7832. (c) Zhang, Y.; Riduan, S. N. *Chem. Soc. Rev.* **2012**, *41*, 2083−2094. (d) Cooper, A. I. *Adv. Mater.* **2009**, *21*, 1291−1295. (e) Thomas, A. *Angew. Chem., Int. Ed.* **2010**, *49*, 8328−8344. (f) Maly, K. E. *J. Mater. Chem.* **2009**, *19*, 1781−1787. (g) Weder, C. *Angew. Chem., Int. Ed.* **2008**, *47*, 448−450. (h) McKeown, N. B.; Budd, P. M. *Chem. Soc. Rev.* **2006**, *35*, 675−683.
(10) Selected examples: (a) Thiel, K.; Zehbe, R.; Roeser, J.; Strauch, P.; Enthaler, S.; Thomas, A. *Polym. Chem.* **2013**, *4*, 1848−1856. (b) Bleschke, C.; Schmidt, J.; Kundu, D. S.; Blechert, S.; Thomas, A. *Adv. Synth. Catal.* **2011**, *353*, 3101−3106. (c) Du, X.; Sun, Y.; Tan, B.; Teng, Q.; Yao, X.; Su, C.; Wang, W. *Chem. Commun.* **2010**, *46*, 970−972.
(11) Selected examples: (a) Ma, H.; Ren, H.; Meng, S.; Sun, F.; Zhu, G. *Sci. Rep.* **2013**, *3*, 2611−2614. (b) Neti, V. S. P. K.; Wu, X.; Deng, S.; Echegoyen. *Polym. Chem.* **2013**, *4*, 4566−4569. (c) Wang, X.-S.; Liu, J.; Bonefont, J. M.; Yuan, D.-Q.; Thallapally, P. K.; Ma, S. *Chem. Commun.* **2013**, *49*, 1533−1535. (d) Totten, R. K.; Kim, Y.-S.; Weston, M. H.; Farha, O. K.; Hupp, J. T.; Nguyen, S. T. *J. Am. Chem. Soc.* **2013**, *135*, 11720−11723. (e) Saha, B.; Gupta, D.; Abu-Omar, M. M.; Modak, A.; Bhaumik, A. *J. Catal.* **2013**, *299*, 316−320. (f) Modak, A.; Nandi, M.; Mondal, J.; Bhaumik, A. *Chem. Commun.* **2012**, *48*, 248−250. (g) Chen, L.; Yang, Y.; Guo, Z.; Jiang, D. *Adv. Mater.* **2011**, *23*, 3149−3154. (g) Shultz, A. M.; Farha, O. K.; Hupp, J. T.; Nguyen, S. T. *Chem. Sci.* **2011**, *2*, 686−689. (h) Chen, L.; Yang, Y.; Jiang, D. *J. Am. Chem. Soc.* **2010**, *132*, 9138−9143. (i) Mackintosh, H. J.; Budd, P. M.; McKeown, N. B. *J. Mater. Chem.* **2008**, *18*, 573−578. (j) Ferrand, Y.; Maux, P. L.; Simonneaux, G. *Tetrahedron: Asymmetry* **2005**, *16*, 3829−3836.
(12) Kadish, K. M.; Smith, K. M.; Guilard, R. *The Porphyrin Handbook*; Academic Press: San Diego, CA, 2000.
(13) (a) Galardon, E.; Le Maux, P.; Simonneaux, G. *J. Chem. Soc., Perkin Trans. 1* **1997**, 2455−2456. (b) Galardon, E.; Le Maux, P.; Simonneaux, G. *Tetrahedron* **2000**, *56*, 615−621.
(14) (a) Mirafzal, B. A.; Cheng, G.; Woo, L. K. *J. Am. Chem. Soc.* **2002**, *124*, 176−177. (b) Chen, Y.; Huang, L.; Zhang, X. P. *Org. Lett.* **2003**, *5*, 2493−2496. (c) Rose, E.; Ren, P.-Z.; Andrioletti, B. *Chem.—Eur. J.* **2004**, *10*, 224−230. (d) Vyas, R.; Gao, G.-Y.; Harden, J. D.; Zhang, X. P. *Org. Lett.* **2004**, *6*, 1907−1910.
(15) Gopalaiah, K. *Chem. Rev.* **2013**, *113*, 3248−3296.
(16) (a) Jiang, J.-X.; Su, F.; Trewin, A.; Wood, C. D.; Campbell, N. L.; Niu, H.; Dickinson, C.; Ganin, A. Y.; Rosseinsky, M. J.; Khimyak, Y. Z.; Cooper, A. I. *Angew. Chem., Int. Ed.* **2007**, *46*, 8574−8578. (b) Jiang, J.-X.; Su, F.; Trewin, A.; Wood, C. D.; Niu, H.; Jones, J. T. A.; Khimyak, Y. Z.; Cooper, A. I. *J. Am. Chem. Soc.* **2008**, *130*, 7710−7722. (c) Jiang, J.-X.; Laybourn, A.; Clowes, R.; Khimyak, Y. Z.; Bacsa, J.; Higgins, S. J.; Adams, D. J.; Cooper, A. I. *Macromolecules* **2010**, *43*, 7577−7582.
(17) (a) Cho, H. C.; Lee, H. S.; Chun, J.; Lee, S. M.; Kim, H. J.; Son, S. U. *Chem. Commun.* **2011**, *47*, 917−919. (b) Chun, J.; Park, J. H.; Kim, J.; Lee, S. M.; Kim, H. J.; Son, S. U. *Chem. Mater.* **2012**, *24*, 3458−3463. (c) Lee, H. S.; Choi, J.; Jin, J.; Chun, J.; Lee, S. M.; Kim, H. J.; Son, S. U. *Chem. Commun.* **2012**, *48*, 94−96. (d) Kang, N.; Park, J. H.; Choi, J.; Jin, J.; Chun, J.; Jung, I. G.; Jeong, J.; Park, J.-G.; Lee, S. M.; Kim, H. J.; Son, S. U. *Angew. Chem., Int. Ed.* **2012**, *51*, 6626−6630. (e) Kang, N.; Park, J. H.; Ko, K. C.; Chun, J.; Kim, E.; Shin, H. W.; Lee, S. M.; Kim, H. J.; Ahn, T. K.; Lee, J. Y.; Son, S. U. *Angew. Chem., Int. Ed.* **2013**, *52*, 6228−6232. (f) Chun, J.; Kang, S.; Lee, S. M.; Kim, H. J.; Son, S. U. *J. Mater. Chem. A* **2013**, *1*, 5517−5523. (g) Park, J. H.; Ko, K. C.; Park, N.; Shin, H.-W.; Kim, E.; Kang, N.; Ko, J. H.; Lee, S. M.; Kim, H. J.; Ahn, T. K.; Lee, J. Y.; Son, S. U. *J. Mater. Chem. A* **2014**, *2*, 7656−7661.
(18) (a) Kang, N.; Park, J. H.; Jin, M.; Park, N.; Lee, S. M.; Kim, H. J.; Kim, J. M.; Son, S. U. *J. Am. Chem. Soc.* **2013**, *135*, 19115−19118. (b) Chun, J.; Kang, S.; Park, N.; Park, E. J.; Jin, X.; Kim, K.-D.; Seo, H. O.; Lee, S. M.; Kim, H. J.; Kwon, W. H.; Park, Y.-K.; Kim, J. M.; Kim, Y. D.; Son, S. U. *J. Am. Chem. Soc.* **2014**, *136*, 6786−6789. (c) Lim, B.; Jin, J.; Yoo, J.; Han, S. Y.; Kim, K.; Kang, S.; Park, N.; Lee, S. M.; Kim, H. J.; Son, S. U. *Chem. Commun.* **2014**, *50*, 7723−7726.
(19) (a) Drouet, S.; Merhi, A.; Yao, D.; Cifuentes, M. P.; Humphrey, M. G.; Wielgus, M.; Olesiak-Banska, J.; Matczyszyn, K.; Samoc, M.; Paul, F.; Paul-Roth, C. O. *Tetrahedron* **2012**, *68*, 10351−10359. (b) Sun, Z.-C.; She, Y.-B.; Zhou, Y.; Song, X.-F.; Li, K. *Molecules* **2011**, *16*, 2960−2970. (c) Delapierre, G.; Duclairoir, F.; Marchon, J.-C. *PCT Int. Appl.* WO 2007048924, 2007.
(20) Skrzypek, D.; Madejska, I.; Habdas, J. *J. Phys. Chem. Solids* **2005**, *66*, 91−97.
(21) Ge, J.; Yin, Y. *Adv. Mater.* **2008**, *20*, 3485−3491.
(22) (a) Baumann, L. K.; Mbuvi, H. M.; Du, G.; Woo, L. K. *Organometallics* **2007**, *26*, 3995−4002. (b) Aviv, I.; Gross, Z. *Synlett* **2006**, *6*, 951. (c) Aiv, I.; Gross, Z. *Chem. Eur. J.* **2008**, *14*, 3995−4005.
(23) It should be noted that the 6 N HCl solution has been used in the workup process for Fe−porphyrin complexes (see the Experimental Section and ref 19b). The retention of $Fe^{III}Cl$ in porphyrin moieties of **H-FePN** during the etching process of inner Fe_3O_4 materials was further confirmed by the absence of a Q band at 660 nm (absorption band of the metal-free porphyrin moiety) in reflectance spectroscopy of **H-FePN**.
(24) (a) Zhu, Z.; Espenson, J. H. *J. Am. Chem. Soc.* **1996**, *118*, 9901−9907. (b) Yang, M.; Wang, X.; Li, H.; Livant, P. *J. Org. Chem.* **2001**, *66*, 6729−6733. (c) Morilla, M. E.; Díaz-Requejo, M. M.; Belderrain, T. R.; Nicasio, M. C.; Trofimenko, S.; Peréz, P. J. *Chem. Commun.* **2002**, 2998−2999. (d) Anding, B. J.; Woo, L. K. *Organometallics* **2013**, *32*, 2599−2607. (e) Xu, B.; Zhu, S.-F.; Zuo, X.-D.; Zhang, Z.-C.; Zhou, Q.-L. *Angew. Chem., Int. Ed.* **2014**, *53*, 3913−3916.
(25) In screening the solvent, the reactions showed 100%, 80%, and 49% conversion of EDA in methylene chloride, hexane, and tolune, respectively. When *tert*-butyl diazoacetate was used instead of EDA, the conversion was 32% in acetone after 20 min.
(26) When 1 mol % of the monomer ($Fe^{III}Cl$−5,10,15,20-tetrakis(4-ethynylphenyl)porphyrin) was used in acetone instead of Fe_3O_4@**FePMN**, the reactions showed 63% and 100% conversion of EDA after 1 and 3 min, respectively.
(27) (a) Kadish, K. M.; Bottomley, L. A.; Brace, J. G.; Winograd, N. *J. Am. Chem. Soc.* **1980**, *102*, 4341−4344. (b) Grosvenor, A. P.; Kobe, B. A.; Biesinger, M. C.; McIntyre, N. S. *Surf. Interface Anal.* **2004**, *36*, 1564−1574.
(28) The detection limit (0.2 ppm) for Fe ions corresponds to 0.0005 times the amount of Fe in the catalyst used.